A Single Transition State Serves Two Mechanisms: An ab Initio Classical Trajectory Study of the Electron Transfer and Substitution Mechanisms in Reactions of Ketyl Radical Anions with Alkyl Halides

Vebjørn Bakken,[†,‡] **David Danovich,**[§] **Sason Shaik,**[*,§] **and H. Bernhard Schlegel**[*,†]

Contributions from the Department of Chemistry, Wayne State University, Detroit, Michigan 48202, and the Department of Organic Chemistry and the Lise Meitner-Minerva Center of Computational Quantum Chemistry, Hebrew University, Jerusalem 91904, Israel

Abstract: Molecular dynamics has been used to investigate the reaction of a series of ketyl anion radicals and alkyl halides, $CH_2O^{\bullet-} + CH_3X$ (X = F, Cl, Br) and $NCCHO^{\bullet-} + CH_3Cl$. In addition to a floppy outer-sphere transition state which leads directly to ET products, there is a strongly bound transition state that yields both electron transfer (ET) and C-alkylated (SUB(C)) products. This common transition state has significant C-- C bonding and gives ET and SUB(C) products via a bifurcation on a single potential energy surface. Branching ratios have been estimated from ab initio classical trajectory calculations. The SUB(C) products are favored for transition states with short C--C bonds and ET for long C--C bonds. ET reactivity can be observed even at short distances of r_{C-C} = ca. 2.4 Å as in the transition state for the reaction $NCCHO^{\bullet-} + CH_3Cl$. Therefore, the ET/SUB(C) reactivity is entangled over a significant range of the C--C distance. The mechanistic significance of the molecular dynamics study is discussed.

Introduction

Much interest has recently been focused on the transformation between electron transfer (ET) and substitution (SUB) mechanisms as the nature of the reactants is gradually varied.[1−5] Particular attention was paid to the question whether the

† Wayne State University.

‡ Permanent address: Department of Chemistry, University of Oslo, P.O. Box 1033 Blindern, N-0315 Oslo, Norway.

§ Hebrew University.

(1) (a) Pross, A. *Acc. Chem. Res.* **1985,** *18,* 212. (b) Kochi, J. K. *Angew. Chem., Int. Ed. Engl.* **1988,** *27,* 1227. (c) Eberson, L. *New J. Chem.* **1992,** *16,* 151. (d) Lund, H.; Daasberg, K.; Lund, T.; Pedersen, S. U. *Acc. Chem. Res.* **1995,** *28,* 313. (e) Eberson, L.; Shaik, S. S. *J. Am. Chem. Soc.* **1990,** *112,* 4484. (f) Savéant, J.-M. *Adv. Phys. Org. Chem.* **1990,** *26,* 1. Savéant, J.-M. *Acc. Chem. Res.* **1993,** *26,* 455. (g) Garst, J. F.; Smith, C. D. *J. Am. Chem. Soc.* **1976,** *98,* 1520. Garst, J. F. *Acc. Chem. Res.* **1971,** *4,* 400. (h) Bilkis, I. I.; Selivanov, B. A.; Shteingarts, V. D. *Res. Chem. Intermed.* **1993,** *19,* 463. (i) Honda, E.; Tokuda, M.; Yoshida, H.; Ogasawara, M. *Bull. Chem. Soc. Jpn.* **1987,** *60,* 851. (j) Eberson, L. *Electron-Transfer Reactions in Organic Chemistry*; Springer-Verlag: Heidelberg, 1987. (k) Chanon, M. *Bull. Chim. Soc. Fr. Part II* **1982,** 197. (l) Zipse, H. *Angew. Chem., Int. Ed. Engl.* **1997,** *36,* 1697. (m) Speiser, B. *Angew. Chem., Int. Ed. Engl.* **1996,** *35,* 2471. (n) Reddy, A. C.; Sastry, G. N.; Shaik, S. *J. Chem. Soc., Perkin Trans. 2,* **1995,** 1717. Reddy, A. C.; Danovich, D.; Ioffe, A.; Shaik, S. *J. Chem. Soc., Perkin Trans. 2* **1995,** 1525. (o) Cho, J. K.; Shaik, S. S. *J. Am. Chem. Soc.* **1991,** *113,* 9890.
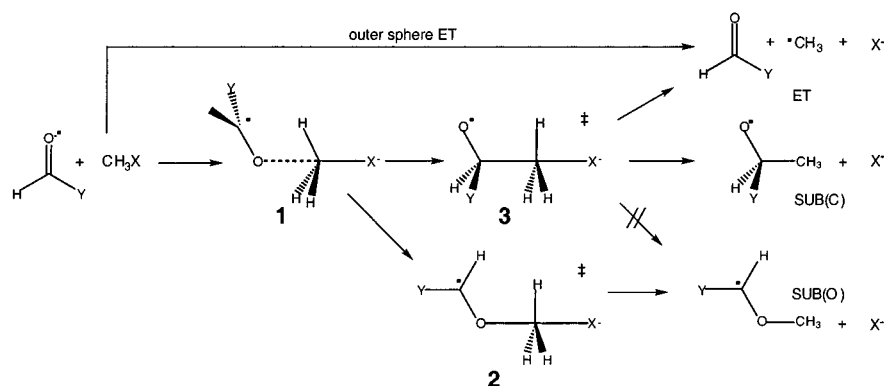
(2) (a) Kimura, N.; Takamuku, S. *J. Am. Chem. Soc.* **1994,** *116,* 4087. Kimura, N.; Takamuku, S. *Bull. Chem. Soc. Jpn.* **1991,** *64,* 2433. (b) Daasberg, K.; Pedersen, S. U.; Lund, H. *Acta Chem. Scand.* **1991,** *45,* 424. (c) Lund, T.; Lund, H. *Acta Chem. Scand.* **1986,** *B40,* 470; **1987,** *B41,* 93. (d) Daasberg, K.; Christensen, T. B. H *Acta Chem. Scand.* **1995,** *49,* 128. (e) Lexa, D.; Savéant, J.-M *J. Am. Chem. Soc.* **1988,** *110,* 7617. (f) Daasberg, K.; Hansen, J. H.; Lund, H. *Acta Chem. Scand.* **1990,** *44,* 711. (g) Daasberg, K.; Lund, H. *Acta Chem. Scand.* **1996,** *50,* 299. (h) Bordwell, F. G.; Harrelson, J. A., Jr. *J. Org. Chem.* **1989,** *54,* 4893. (i) Bordwell, F. G.; Harrelson, J. A., Jr. *J. Am. Chem. Soc.* **1989,** *111,* 1052. (j) Tolbert, L. M.; Bedlek, J.; Terapane, M.; Kowalik, J. *J. Am. Chem. Soc.* **1997,** *119,* 2291. (k) Haberfild, P. *J. Am. Chem. Soc.* **1995,** *117,* 3314.

(3) (a) Sastry, G. N.; Shaik, S. *J. Am. Chem. Soc.* **1995,** *117,* 3290. (b) Sastry, G. N.; Danovich, D.; Shaik, S. *Angew. Chem., Int. Ed. Engl.* **1996,** *35,* 1098. (c) Sastry, G. N.; Shaik, S. *J. Phys. Chem.* **1996,** *100,* 12241. (d) Shaik, S.; Danovich, D.; Sastry, G. N.; Ayala, P. Y.; Schlegel, H. B. *J. Am. Chem. Soc.* **1997,** *119,* 9237. (e) Sastry, G. N.; Shaik, S. *J. Am. Chem. Soc.* **1998,** *120,* 2131. (f) Shaik, S.; Shurki, A. *Angew. Chem., Int. Ed. Engl.* **1999,** *38,* 587.

mechanisms are mutually exclusive with distinct transition states or whether the mechanisms are related, with transition states that form a continuum of related structures.[1a,d,f,2b−g] Still other questions concerned the degree of bonding between the nucleophile and electrophile moieties in the ET transition state (ET-TS).[1a−f,j,2a,j] In one extreme, electron transfer can occur via a weakly bound outer-sphere-type species (bonding ≤1 kcal/mol) that involves hopping between two potential energy surfaces. In the other extreme the reaction can proceed on a single electronic surface via a tightly bound species with distinct stereochemical constraints.[1e,l] Clearly, the entanglement of the two mechanisms and their crossover,[3d−f] the occasional similarity of structure−reactivity relationships exhibited in them,[2a] and their importance as two prototypical mechanisms of chemical reactivity by and large make their relationship a fundamental issue. A recent intriguing issue is the notion[1l,3d−f,5] that in some cases, a single transition state can lead to both ET and SUB products via bifurcation on a single, ground-state potential energy surface. Should this be the case, some fundamental mechanistic concepts of physical organic chemistry would have to be reconsidered, chiefly the concept of the microscopic reversibility of the reaction mechanism.

The reactions between ketyl radical anions and alkyl halides exhibit this richness of problems[2a,3−5] and provide thereby ideal targets for a theoretical investigation of the mechanistic question by means of molecular dynamics. Thus, ketyl radical anions can react with alkyl halides via outer-sphere ET or via two different transition states that involve partial bond formation.[3,4] Outer-sphere ET may involve a weak interaction, but is not expected to have a significant orientational preference.[4] The other reactions can proceed via a reactant complex, **1**, in which the oxygen interacts with the alkyl carbon. Substitution by oxygen, SUB(O), occurs by way of a separate S_N2 transition

(4) Bertran, J.; Gallardo, I.; Moreno, M.; Savéant, J.-M. *J. Am. Chem. Soc.* **1996,** *118,* 5737.

(5) Yamataka, H.; Aida, M.; Dupuis, M. *Chem. Phys. Lett.* **1999,** *300,* 583.

Scheme 1

state, **2**, in which the oxygen lone pair displaces the halide in the usual backside approach.[3,4] The transition state **3** involving attack by the carbon of the ketyl radical anion is the one of central interest to the studies of mechanistic crossover. Depending on the substituents, the ground-state potential energy surface can lead from this transition state to both ET products and substitution at carbon, SUB(C),[3,4] and in some cases may also yield substitution at oxygen. *Therefore, this transition state serves simultaneously for several distinct mechanisms.* Reactions between ketyl radical anions and alkyl halides have been studied both experimentally and theoretically.[2-5] The ab initio studies[3] demonstrate that the C--C bonded transition state, **3**, gives either ET or SUB(C) products depending on the C−C distance; the reaction path leads to ET for $r_{C-C} \geq$ ca. 2.45 Å and SUB(C) if r_{C-C} is shorter.[3e-f] Thus, changing to a less electronegative halide switches the mechanism from SUB(C) to ET. Changing to radical anions that are poorer electron donors favors SUB-(C). Making the alkyl halide bulkier or making the transition state more strained favors the ET mechanism.[3d,e] An investigation of the shape of the potential surface[3d] has suggested that the ET/SUB(C) mechanisms are both nascent from the same transition structures, and therefore their reactivities should be strongly entangled. The need for dynamics has been pointed out by a number of authors,[1l,3d-f] and the first dynamics calculations have been reported recently for the reaction $CH_2O^{\bullet-}$ + CH_3Cl.[5] In the present work, we use ab initio classical trajectories on the Born−Oppenheimer surface to study branching ratios in an extended reaction series, $CH_2O^{\bullet-}$ + CH_3X (X = F, Cl, Br) and $NCCHO^{\bullet-}$ + CH_3Cl. We have calculated a variety of individual trajectories with a range of initial conditions to help understand the factors contributing to the branching ratios, and we have examined thermal ensembles of trajectories to obtain estimates of the branching ratios.

Theory

General Considerations of Approaches for Studying Reaction Mechanisms. Generally, reaction path following[6] is used to classify the reaction mechanism, but sometimes, as in the reactions of Scheme 1, the results may be ambiguous. For the same reaction, path following can give a different result in internal coordinates than in mass-weighted coordinates.[3b-d] Changing the level of theory from spin unrestricted calculations to spin restricted (e.g. UHF to ROHF) can also affect the outcome of reaction path following,[3b-d] even though the topology of the surface remains the same. The calculation of
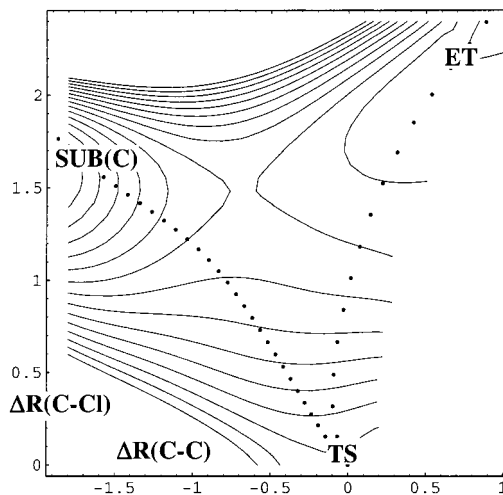
(6) Schlegel, H. B. In *Encyclopedia of Computational Chemistry*; Schleyer, P. v. R., Allinger, N. L., Clark, T., Gasteiger, J., Kollman, P. A., Schaefer, H. F., III, Schreiner, P. R., Eds.; Wiley: Chichester, 1998; p 2432 and references therein.

Figure 1. Contour plot of a cross-section of the potential energy surface for $CH_2O^{\bullet-}$ + CH_3Cl,[3d] showing that the surface bifurcates into ET and SUB(C) channels as it descends from the transition state.

vibrational frequencies along the path reveals a bifurcation in the path as it descends from the transition state toward products.[3c,d] A cross-section of the surface for $CH_2O^{\bullet-}$ + CH_3Cl, Figure 1, shows a low ridge separating the product valleys for electron transfer and substitution at carbon.[3d] The presence of such a bifurcation can explain why path following can lead to different results with small changes in the level of theory. Bifurcation of the potential energy surface into two product valleys can also explain how the mechanism can change as substituents are varied. The question of which mechanism dominates depends on the relative rates of formation of the products.

The rate of a reaction can be estimated by transition state theory from the energy, structure, and vibrational frequencies of the transition state.[7] Reaction path following can identify with some certainty the reactants and products connected by the transition state, unless the path branches. If the branching occurs before the transition state, there will be a separate transition state for each branch, and transition state theory can be used to estimate the relative rates. If the branching occurs after the transition state, as in the present case (see Figure 1), the branching ratio cannot be determined by transition state theory, but depends on the nature of the potential energy surface as it descends from the transition state toward the different products. Branching in the reaction path can be detected by analyzing the vibrational frequencies perpendicular to the path.[8] The valley-ridge inflection point (VRI) is where one of the perpen-

(7) Steinfeld, J. I.; Francisco, J. S.; Hase, W. L. *Chemical Kinetics and Dynamics*; Prentice Hall: Englewood Cliffs, 1989.

dicular frequencies goes to zero, and marks the place where a valley turns into a ridge indicating branching of the potential energy surface. As molecules move on the potential energy surface, they do not follow the steepest descent reaction path, but explore much wider regions of the potential energy surface. Thus if the branching occurs after the transition state, the system must be studied with molecular dynamics. If there are large differences in the reaction paths leading to different products, then approximate methods of estimating the outcome of dynamics may be sufficient.[9] For the more subtle differences in the potential energy surface, as in the present case, molecular dynamics needs to be considered explicitly.

For the reactions in Scheme 1, the molecular dynamics can probably be modeled adequately by classical trajectory calculations;[10] quantum effects should be small since the reaction occurs on a single potential energy surface and most of the motion involves heavy groups. For economic reasons, classical trajectory calculations have traditionally been carried out on global analytical surfaces.[11] However, it is difficult to construct accurate surfaces for these reactions because of the many degrees of freedom and the complicated nature of bond making/breaking in the transition state region. For small systems, one can compute classical trajectories directly from ab initio electronic structure calculations.[12]

There are two approaches to ab initio molecular dynamics: Car−Parrinello and Born−Oppenheimer. In the Car−Parrinello approach,[13] both the wave function and the nuclei are propagated by the appropriate equations of motion. In the Born−Oppenheimer approach,[12] the wave function is converged at every step and the molecule is propagated on a well-defined potential energy surface. Since branching in these reactions depends on subtle details of the potential energy surface, we choose the latter approach.

Methodology

Technical Methods. The classical equations of motion were integrated by using a Hessian-based predictor−corrector algorithm.[14,15] The energy, gradient, and Hessian (second derivative or force constant

Figure 2. Optimized geometries of the transiton states for the reactions of $CH_2O^{\bullet-}$ + CH_3F, CH_3Cl, and CH_3Br as well as $NCCHO^{\bullet-}$ + CH_3-Cl (for $CH_2O^{\bullet-}$ + CH_3Cl, HF/3-21G, HF/6-31G*, HF/6-31+G*, MP2/6-31+G*, and QCISD/6-31G*, listed from top to bottom, and HF/3-21G for the others). Arrows indicate the transition vectors.

matrix) are obtained at the beginning of a trajectory step. For the predictor phase, the classical equations of motion are integrated on this local quadratic surface for a fixed distance. The energy, gradient, and Hessian are calculated at the endpoint of the predictor step. The energy, gradient, and Hessian at the beginning and end of the step are fitted to a 5th order polynomial surface. A corrector step is then taken by integrating the equations of motion on the 5th order polynomial surface. The energy, gradient, and Hessian at the end of the predictor step are used for the beginning of the next step. Details of the integration algorithm have been published elsewhere.[14,15] The ab initio work per step is the same as the local quadratic model used by Helgaker et al.,[16] but the step size can be increased by an order of magnitude without loss of accuracy. Because the potential energy surface is fairly smooth, it is possible to update the Hessian rather than recalculate it at each step.[15] With 5 updates before recalculating the Hessian, the computational work is reduced by an additional factor of 3. The ab initio classical trajectory calculations were carried out with the development version of Gaussian 98.[17]

The trajectories were started at the optimized transition states shown in Figure 2, and the initial conditions were chosen to correspond to a reaction at 298 K. Motion along the transition vector in the direction toward products was sampled from a thermal distribution. The remaining vibrational modes were given zero-point vibrational energy plus sampled thermal energy; the rotational energy for the system was also based on sampling from a thermal distribution of a symmetric top. The trajectories were integrated with step sizes ranging from 0.075 to 0.20 $amu^{1/2}$ bohr. The step sizes are chosen so that the total energy is conserved to better than 10^{-5} hartree (0.006 kcal/mol). Total angular momentum is conserved to better than $10^{-9}\hbar$. Trajectories were stopped when the distances between fragments were larger than ca. 12 bohr (corresponding to 100−500 fs and up to 1300 integration steps) or when the maximum number of steps was exceeded (350−500 fs). The Hartree−Fock level of theory has been found to be quite satisfactory for calculating classical trajectories to analyze the molecular dynamics

(8) For discussions of bifurcations and algorithms to handle reaction path branching see: Valtazanos, P.; Ruedenberg, K. *Theor. Chim. Acta* **1986**, *69*, 281. Krauss, W. A.; Depristo, A. E. *Theor. Chim. Acta* **1986**, *69*, 309. Basilevsky, M. V. *Theor. Chim. Acta* **1987**, *72*, 63. Taketsugu, T.; Hirao, K. *J. Chem. Phys.* **1993**, *99*, 9806. Taketsugu, T.; Hirao, K. *Theomchem* **1994**, *310*, 169. Baker, J.; Gill, P. M. W. *J. Comput. Chem.* **1988**, *9*, 465. Simons, J. *Int. J. Quantum Chem.* **1993**, *48*, 211. Simons, J. *Int. J. Quantum Chem.* **1993**, *48*, 309. Bosch, E.; Moreno, M.; Lluch, J.; Bertran, J. *Chem. Phys. Lett.* **1989**, *160*, 543. Taketsugu, T.; Tajima, N.; Hirao, K. *J. Chem. Phys.* **1996**, *105*, 1933.

(9) Perterson, T. H.; Carpenter, B. K. *J. Am. Chem. Soc.* **1992**, *114*, 766. Lyons, B. A.; Pfeifer, J.; Peterson, T. H.; Carpenter, B. K. *J. Am. Chem. Soc.* **1993**, *115*, 2427.

(10) Bunker, D. L. Classical Trajectory Methods. In *Methods Comput. Phys.* **1971**, *10*, 287. Raff L. M.; Thompson, D. L. In *Theory of Chemical Reaction Dynamics*; Baer, M., Ed.; CRC Press: Boca Raton, 1985. *Advances in Classical Trajectory Methods*; Hase, W. L., Ed.; JAI Press: Greenwich, 1992; and references therein. Thompson, D. L. In *Encyclopedia of Computational Chemistry*; Schleyer, P. v. R., Allinger, N. L., Clark, T., Gasteiger, J., Kollman, P. A., Schaefer, H. F., III, Schreiner, P. R., Eds.; Wiley: Chichester, 1998; p 3056 and references therein.

(11) Schatz, G. C. *Rev. Mod. Phys.* **1989**, *61*, 669. Schatz, G. C.; Schatz, G. C. In *Advances in Molecular Electronic Structure Theory*; Dunning, T. H., Ed.; JAI Press: London, 1990.

(12) For a recent review of ab initio classical trajectory methods and a comparison of Born−Oppenheimer and Car−Parrinello methods see: Bolton, K.; Hase, W. L.; Peshlherbe, G. H. In *Modern Methods for Multidimensional Dynamics Computation in Chemistry;* Thompson, D. L., Ed.; World Scientific: Singapore, 1998.

(13) Car, R.; Parrinello, M. *Phys. Rev. Lett.* **1985**, *55*, 2471. Tuckerman, M. E.; Ungar P. J.; von Rosenvinge, T.; Klein, M. L. *J. Phys. Chem.* **1996**, *100*, 12878 and references therein.

(14) (a) Chen, W.; Hase, W. L.; Schlegel, H. B. *Chem. Phys. Lett.* **1994**, *228*, 436. (b) Millam, J. M.; Bakken, V.; Chen, W.; Hase, W. L.; Schlegel, H. B. *J. Chem. Phys.* **1999**, *111*, 3800.
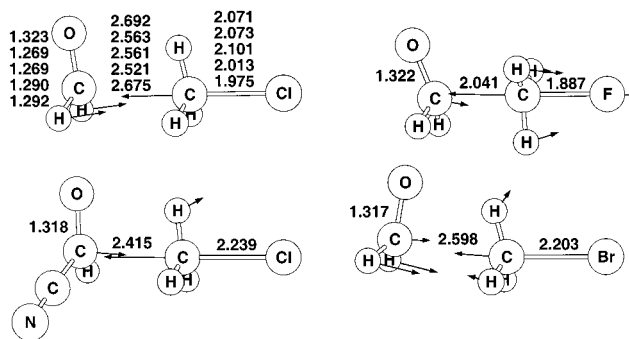
(15) Bakken, V.; Millam, J. M.; Schlegel, H. B. *J. Chem. Phys.* **1999**, *111*, 8773.

(16) Helgaker, T.; Uggerud, E.; Jensen, H. J. A. *Chem. Phys. Lett.* **1990**, *173*, 145. Uggerud, E.; Helgaker, T. *J. Am. Chem. Soc.* **1992**, *114*, 4265. Bueker, H.-H.; Helgaker, T.; Ruud, K.; Uggerud, E. *J. Phys. Chem.* **1996**, *100*, 15388. Bueker, H. H.; Uggerud, E. *J. Phys. Chem.* **1995**, *99*, 5945. Ruud, K.; Helgaker, T.; Uggerud, E. *Theochem.-J Mol. Struct.* **1997**, *393*, 59. Oiestad, E. L.; Uggerud, E. *Int. J. Mass Spectrom.* **1997**, *165*, 39.

(17) Gaussian 98, M. J. Frisch, G. W. Trucks, H. B. Schlegel, G. E. Scuseria, M. A. Robb, J. R. Cheeseman, V. G. Zakrzewski, J. A. Montgomery, R. E. Stratmann, J. C. Burant, S. Dapprich, J. M. Millam, A. D. Daniels, K. N. Kudin, M. C. Strain, Ö. Farkas, J. Tomasi, V. Barone, M. Cossi, R. Cammi, B. Mennucci, C. Pomelli, G. A. Petersson, P. Y. Ayala, A. D. Rabuck, K. Raghavachari, Q. Cui, K. Morokuma, J. B. Foresman, J. Cioslowski, J. V. Ortiz, V. Barone, B. B. Stefanov, G. Liu, A. Liashenko, P. Piskorz, W. Chen, M. W. Wong, J. L. Andres, E. S. Replogle, R. Gomperts, R. L. Martin, D. J. Fox, T. Keith, M. A. Al-Laham, A. Nanayakkara, C. Y. Peng, M. Challacombe, P. M. W. Gill, B. Johnson, and J. Pople, Gaussian, Inc.: Pittsburgh, PA, 1998.
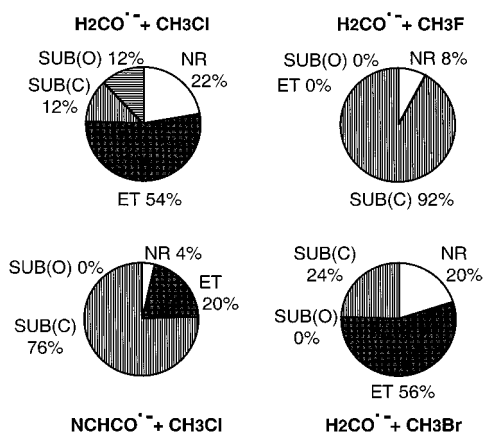
Figure 3. Branching ratios for the reactions of $CH_2O^{\bullet-}$ + CH_3F, CH_3-Cl, and CH_3Br as well as $NCCHO^{\bullet-}$ + CH_3Cl obtained from trajectories computed at the HF/3-21G level of theory.

of formaldehyde photodissociation,[14a,18] S_N2 reactions,[19] and radical additions to multiple bonds.[20] Trajectories calculated at the HF/6-31+G* level[5] show features similar to the HF/6-31G* trajectories in the present work. Addition of diffuse functions and electron correlation did not alter the geometry of the transition state significantly[3c] (see Figure 2). Earlier work also showed that barrier heights varied little with the level of theory.[3c] These observations indicate that the HF/6-31G* level of theory is sufficient for the present study. For $CH_2O^{\bullet-}$ + CH_3Cl, the branching ratios for ET product are very similar at HF/3-21G and HF/6-31G* (see below), suggesting that qualitative trends can be obtained adequately at HF/3-21G. Thus the HF/3-21G level of theory was used to calculate the classical trajectories for $CH_2O^{\bullet-}$ with CH_3F, CH_3Cl, and CH_3Br as well as for $NCCHO^{\bullet-}$ + CH_3Cl.

To gain a complementary qualitative insight into the effects of a wider range of starting conditions on the dynamics of the branching ratios, the $CH_2O^{\bullet-}$ + CH_3Cl reaction was also explored using trajectories calculated with GAMESS-US[21] (using the dynamic reaction path[22] option). The trajectories were calculated using the HF/6-31G* level of theory with selected amounts of kinetic energy put into the transition mode, with and without zero-point energy in the rest of the vibrational modes. The trajectories were propagated for 500 fs with a time step of 0.1 fs; total energy was conserved to 5×10^{-5} hartree.

Results

The classical trajectories were calculated for a set of reactions which provide a range of mechanistic variation from SUB(C) all the way to ET. The transition state structures are summarized in Figure 2 and are seen to vary primarily in their C—C distances. The branching ratios from a statistical sample of trajectories computed at the HF/3-21G level of theory are summarized in Figure 3 and discussed below.

$CH_2O^{\bullet-}$ + CH_3Cl: In a previous study, Yamataka et al.[5] used the HF/6-31+G* level of theory to calculate 9 trajectories starting from the transition state with randomly selected velocities consistent with $T = 298$ K. They found three gave

(18) Li, X.; Millam, J. M.; Schlegel, H. B. *J. Chem. Phys.* **2000**, *113*, 10062.
(19) Li, G. S.; Hase, W. L. *J. Am. Chem. Soc.* **1999**, *121*, 7124.
(20) Bolton, K.; Hase, W. L.; Schlegel, H. B.; Song, K. *Chem. Phys. Lett.* **1988**, *288*, 621. Bolton, K.; Schlegel, H. B.; Hase, W. L.; Song, K. *Phys. Chem. Chem. Phys.* **1999**, *1*, 999.
(21) GAMESS-USA, revision May 1998, Schmidt, M. W.; Baldridge, K. K.; Boatz, J. A.; Elbert, S. T.; Gordon, M. S.; Jensen, J. H.; Koseki, S.; Matsunaga, N.; Nguyen, K. A.; Su, S. J.; Windus, T. L.; Dupuis, M.; Montgomery, J. A.; see e.g.: Schmidt, M. W.; Baldridge, K. K.; Boatz, J. A.; Elbert, S. T.; Gordon, M. S.; Jensen, J. H.; Koseki, S.; Matsunaga, N.; Nguyen, K. A.; Su, S. J.; Windus, T. L.; Dupuis, M.; Montgomery, J. A. *J. Comput. Chem.* **1993**, *14*, 1347.
(22) Gordon, M. S.; Chaban, G.; Taketsugu, T, *J. Phys. Chem.* **1996**, *100*, 11512.

ET products and three gave SUB(C) products, but not enough trajectories were studied to estimate branching. Before calculating an appropriate statistical sample to obtain an estimate of the branching ratios, we decided to explore the qualitative effects of different starting conditions on the mechanism of the reaction. Twenty trajectories were computed with 7−70 kcal/mol kinetic energy in the transition vector, and with or without zero-point energy in the remaining modes. When up to 50 kcal/mol was put in the transition vector in the forward direction, SUB(C) products were obtained; with more than 50 kcal/mol, ET products were formed. With zero-point energy added to the other modes, ET products were favored even at lower energies. For motion in the reverse direction, the system returned to reactants if the transition vector was given less than ca. 50 kcal/mol. With more than ca. 50 kcal/mol, SUB(O) products were formed after passing through the initial reactant cluster, **1** (see Scheme 1).

To obtain an estimate of the branching ratios, we used the Hessian-based predictor−corrector algorithm[14,15] to calculate an ensemble of 20 trajectories at HF/6-31G* and 50 trajectories at HF/3-21G with the initial conditions for each chosen from a thermal distribution at 298 K. In both cases, ET was the major product (55% in HF/6-31G* and 54% in HF/3-21G) with SUB-(C) being the second most abundant product (40% in HF/6-31G* and 12% in HF/3-21G), and SUB(O) relatively minor (0% in HF/6-31G* and 12% in HF/3-21G). The time required to reach products varied from 100 to 500 fs, with ET trajectories on average requiring almost twice as long as SUB(C). Some trajectories started as SUB(C) but dissociated to ET (2 out of 50 at HF/3-21G). Similar behavior was reported by Yamataka et al.[5] for one of their trajectories. The trajectories leading to SUB(C) and ET proceeded to products directly from the same transition state (the C--C type transition state **3** in Scheme 1). Those leading to SUB(O) products passed near the reactant cluster, **1**, and then to products via a different transition state (the O--C type transition state **2** in Scheme 1). The fraction of trajectories leading to SUB(O) is anomalously high at the HF/3-21G level because the barrier between reactant cluster **2** and the SUB(O) products is small or nonexistent at HF/3-21G. Some of the SUB(O) trajectories had sufficient energy so that integration for a longer time resulted in dissociation into ET products. Compared to the average over all trajectories, those leading to ET typically had more energy in the transition vector initially than the average; SUB(O) trajectories generally had less energy in the transition vector than SUB(C) trajectories. A number of trajectories were deflected back to reactants (no reaction (NR): 22% in HF/3-21G and 5% in HF/6-31G*). These trajectories usually had significantly less energy in the transition vector and more rotational energy than the average.

$CH_2O^{\bullet-}$ + CH_3F: Of the 25 trajectories studied at the HF/3-21G level, 92% lead to SUB(C), while the rest (8%) returned to reactants. None of the trajectories lead to either ET or SUB-(O) products. We note that in many trajectories, the expelled F^- eventually came around to abstract an H from the CH_2 group.

$CH_2O^{\bullet-}$ + CH_3Br: The corresponding transition state has the longest C—C bond length in our series. The results are quite similar to $CH_2O^{\bullet-}$ + CH_3Cl, with the exception that no SUB-(O) products were observed. Thus, of the 25 trajectories at HF/3-21G, 56% gave ET products, while 24% ended in SUB(C) products, and 20% of the trajectories were deflected back to reactants.

$NCCHO^{\bullet-}$ + CH_3Cl: The transition state for this reaction has an intermediate C—C bond length, between those for $CH_2O^{\bullet-}$ + CH_3F and $CH_2O^{\bullet-}$ + CH_3Cl. In our previous paper[3d] it was concluded that the reaction with $NCCHO^{\bullet-}$ should give

SUB(C) exclusively. The trajectory calculation at HF/3-21G showed, however, that of the 25 trajectories 20% lead to ET products, while the majority, 76%, gave SUB(C) products. The rest, 4%, were deflected back to reactants.

Discussion

The above results highlight the entangled reactivity of substitution and electron-transfer mechanisms via a single transition state that possesses C--C bonding of significant magnitude.[3d] The formation of O-alkylation products, SUB(O), by way of a C--C bonded TS is quite intriguing. Kimura[2a] has reasoned from his experimental investigation with 1-benzoyl-ω-haloalkane that the ET and SUB(O) products share a common transition state structure. If this is indeed the case, then the classical trajectories results suggest that this transition state should be the C--C bonded species. In addition to being formed by a direct reaction via an O--C type transition state **2**, the exploratory trajectory calculations indicate that the SUB(O) products can also be formed when the system is deflected back from the C--C type transition state, **3**, to the reactant cluster, **1**. If the kinetic energy is sufficient, this cluster, which possesses an O--C interaction, can surmount the corresponding barrier of the O--C type transition state[3] **2** to produce the SUB(O) products. We therefore conclude that the C--C bonded transition state, **3**, is connect directly only to the ET and SUB(C) products.[3d]

The exploratory trajectory calculations provide some insight into the energy factor involved in setting the ET/SUB(C) branching ratio, and into the interplay between the shape of the potential energy surface on one hand and the kinetic energy of reacting species on the other hand. When substantial amounts of kinetic energy are deposited in the transition vector in the forward direction, more ET is observed as more energy is available, both with and without zero-point energy in the remaining vibrational modes. Analysis of the thermal ensemble of trajectories reveals the same trend, with trajectories leading to ET products typically having more energy in the transition vector than those leading to other products or those resulting in no reaction. When the transition vector is highly energized, the recoil mechanism which separates the TS into ET fragments, becoming increasingly more activated. As seen from the transition vector in Figure 2, the two hydrogen substituents of the formaldehyde flap against the methyl group in opposition to the C--C approach result in a recoil of the $H_2C=O$ moiety and lengthening of both the C—C and C—Cl bonds. The flapping motion represents, in fact, a chemically simple mechanism by which the bonded TS loses its C--C bonding. Since the carbonyl group undergoes pyramidalization by C--C bonding in the TS (see Figure 2), the flapping mode also serves to restore the planarity of the carbonyl as required by the structure of the ET product. Thus, increasing the activation of the transition mode sends the system down the ET valley with increasing momentum, so that mostly ET products are observed.

For the thermal ensembles, the classical trajectory results exhibit a rough correlation between the ET/SUB(C) branching ratio and the r_{C-C} distance at the transition state. As the distance gets shorter the branching ratio decreases and becomes virtually zero at r_{C-C} = ca. 2.0 Å, which correspond to the reaction with CH_3F. This trend has been deduced from experimental[1d] data for analogous reactions and was predicted theoretically based on ab initio calculations of structures and reaction paths.[3b,d−f] Thus, as expected, the stronger the bonding, the less ET reactivity is observed. However, less expected and certainly intriguing is the result that ET reactivity can be observed even at short distances of r_{C-C} = ca. 2.4 Å, the C--C bond length in

the transition state for the reaction $NCCHO^{•−} + CH_3Cl$. Therefore, the ET/SUB(C) reactivity is entangled over a significant range of the C--C distance, and the maximum allowable bonding in the ET transition state can be very robust, exceeding 14 kcal/mol.[23]

The entangled reactivity has a number of consequences. First, the observation of an excess of inversion of configuration in C—C alkylated products produced from reactions of anion radicals and, e.g., 2-octyl halides,[1d,24] may well be the result of a single transition state that partitions into ET and SUB(C) products, by analogy to the molecular dynamics results. In fact, the amount of enantiomeric excess in such reactions can serve as a measure of the bonding in the ET-TS. An interplay of experiment and theory appears to be the best way to elucidate this fundamental issue of bonding in the ET-TS. Furthermore, experimental determination of kinetic isotope[3a] effect for dissociative ET processes coupled with studies of conformationally locked systems[3e] may enable one to probe the bonding of the ET-TS directly.

Conclusions

Molecular dynamics studies on a series of ketyl anion radicals and alkyl halides (Scheme 1) show that a single transition state with significant C--C bonding leads to both electron transfer (ET) and C-alkylated (SUB(C)) products via bifurcation on a single potential energy surface. Thus, in addition to the floppy outer-sphere transition state that yields ET products, there is also a strong bond TS which leads to ET products.

The mechanistic significance of the surface bifurcation is that the common assumption of microscopic reversibility of the mechanism, made in studies and teachings of reaction mechanism, is not generally valid. Since this is a fundamental issue in reaction mechanisms, it certainly merits both experimental and theoretical characterization. A serious stumbling block is the lack of experimental probes for such surface bifurcations, and one hopes that the new femtosecond experimental techniques will eventually provide such probes. On the side of theory, more extensive reaction dynamic studies, including medium effect, can hopefully reveal additional features of the bifurcation issue and suggest meaningful experimental ways for probing these effects. This is an example where the interplay of theory and experiment is essential to lead to a better mechanistic understanding.

(23) Based on the equation derived in: Rauhut, G.; Clark, T., *J. Chem. Soc., Faraday Trans.* **1994**, *90*, 1783.
(24) Malissard, M.; Mazaleyrat, J.-P.; Welwart, Z. *J. Am. Chem. Soc.* **1977**, *99,* 6933. Herbert, E.; Mazaleyarat, J.-P.; Welvart, Z.; Nadjo, L.; Savéant, J.-M. *New J. Chem.* **1985**, *9*, 75.